metals

MDPI

Article

Distribution Ratio of Sulfur between CaO-SiO_2-Al_2O_3-Na_2O-TiO_2 Slag and Carbon-Saturated Iron

Kanghui Zhang, Yanling Zhang * and Tuo Wu

State Key Laboratory of Advanced Metallurgy, University of Science and Technology Beijing, Beijing 100083, China; kanghuiz@126.com (K.Z.); wutuo90@163.com (T.W.)

* Correspondence: zhangyanling@metall.ustb.edu.cn; Tel.: +86-10-8237-5191

Received: 28 November 2018; Accepted: 12 December 2018; Published: 15 December 2018

Abstract: To explore the feasibility of hot metal desulfurization using red mud, the sulfur distribution ratio (L_S) between CaO-SiO_2-Al_2O_3-Na_2O-TiO_2 slag and carbon-saturated iron is evaluated in this paper. First, the theoretical liquid areas of the CaO-SiO_2-Al_2O_3 (-Na_2O-TiO_2) slag are discussed and the fluxing effects of Al_2O_3, Na_2O, and TiO_2 are confirmed. Then, L_S is measured via slag-metal equilibrium experiments. The experimental results show that L_S significantly increases with the increase of temperature, basicity, and Na_2O content, whereas it decreases with the increase of Al_2O_3 and TiO_2 content. Na_2O in the slag will volatilize with high temperatures and reducing conditions. Furthermore, based on experimental data for the sulfur distribution ratio between CaO-SiO_2-Al_2O_3-Na_2O-TiO_2 slag and the carbon-saturated iron, the following fitting formula is obtained: $\log L_S = 45.584\Lambda + \frac{10568.406-17184.041\Lambda}{T} - 8.529$

Keywords: sulfur distribution ratio; liquid area; carbon-saturated iron

1. Introduction

Sulfur often deteriorates metal properties [1,2], especially metals' toughness. To realize the deep desulfurization of steel [3,4], the process of hot metal desulfurization has become an economical and efficient method [2]. During this process, traditional lime-based slag has a high melting point. Therefore, CaF_2 is widely added as an additive to decrease the melting point and improve the solubility of lime [5]. However, because CaF_2 is toxic to the environment and human health, its use has been strictly restricted [6]. Hence, a desulfurizing slag with a much lower melting point, especially under conditions of high basicity, is required. Previous research [5–12] showed that other additives such as Al_2O_3, Na_2O, and TiO_2, could improve the desulfurization efficiency of lime-based slag. Niekerk and Dippenaar [5] determined that the Na_2O equivalent of CaO was 0.30, and adding Na_2O could significantly increase the sulfide capacity of silicate and lime-based slag. Pak and Fruehan [6] reported that the addition of Na_2O lowered the melting point and improved the fluidity of lime-based slag. Zhang's experiments [7] obtained good slag fluidity and a much better separation between the slag and the melt phases, attributed to the fact that Al_2O_3 and Na_2O could act as a flux and decrease the melting point of the slag. Yajima et al. [8] found that, with the addition of Al_2O_3 to the CaO-SiO_2-FeO_x slag system at an oxygen partial pressure of 1.8×10^{-3} Pa, the liquid areas were enlarged. Park et al. and Sohn et al. [10,11] confirmed that TiO_2 decreased the viscosity of blast furnace slag by depolymerizing the slag structure.

Red mud is the residue discharged by the aluminum industry after the extraction of alumina. In addition to CaO, there is an abundance of Al_2O_3, Na_2O, and TiO_2 in red mud. However, it is piled up, pollutes the environment, and increases the burden on enterprises. The sulfur distribution

ratio between CaO-SiO_2-Al_2O_3-Na_2O-TiO_2 slag and carbon-saturated iron is examined in this study to explore the feasibility of hot metal desulfurization using red mud. First, the liquid areas of the CaO-SiO_2-Al_2O_3 slag system, along with the effects of Al_2O_3, Na_2O, and TiO_2, are investigated thermodynamically using FactSage7.0 software. Then, the sulfur distribution ratio between these slag systems and carbon-saturated iron is examined using an equilibrium experiment in the laboratory.

2. Liquid Areas of the CaO-SiO_2-Al_2O_3 (-Na_2O-TiO_2) Slag System

The liquid areas of CaO-SiO_2-Al_2O_3 slag, simulated by the FactSage7.0 software (developed by CRCT, Montreal, QC, Canada and GTT-Technologies, Herzogenrath, Germany), are shown in Figure 1. Figure 1a shows that the liquid areas at 1400 °C, 1500 °C, and 1600 °C account for about 1/11, 1/4, and 1/2 of the whole diagram area, respectively. This indicates that high temperature is beneficial to the melting of slag. In Figure 1a, there are three lines that correspond to the CaO/SiO_2 of 0.25, 1, and 4, respectively. When CaO/SiO_2 is constant, the melting point of the slag decreases at first and then increases with an increase of Al_2O_3 content, indicating that adding Al_2O_3 can promote the melting of slag at low concentrations, whereas melting deteriorates above a certain content of Al_2O_3. When CaO/SiO_2 is 0.25, 1, and 4, the critical value of Al_2O_3 content is 13.7–19.3%, 15.3–19.1%, and 36.1–43.4%, respectively. Therefore, Al_2O_3 has the effect of a flux, but its concentration should be controlled. Figure 1b,c show the effects of Na_2O and TiO_2 on the liquid areas of CaO-SiO_2-Al_2O_3 slag at 1500 °C, respectively. Figure 1d shows the effect of a Na_2O and TiO_2 mixture (denoted as "NT") at a mass ratio of Na_2O/TiO_2 = 2:1 on the liquid areas of CaO-SiO_2-Al_2O_3 slag at 1500 °C. The liquid areas become enlarged with the increase of Na_2O, TiO_2, and NT content, showing that these additives could all promote the melting of the slag. However, Na_2O and NT could promote the melting of the slag more effectively than TiO_2.

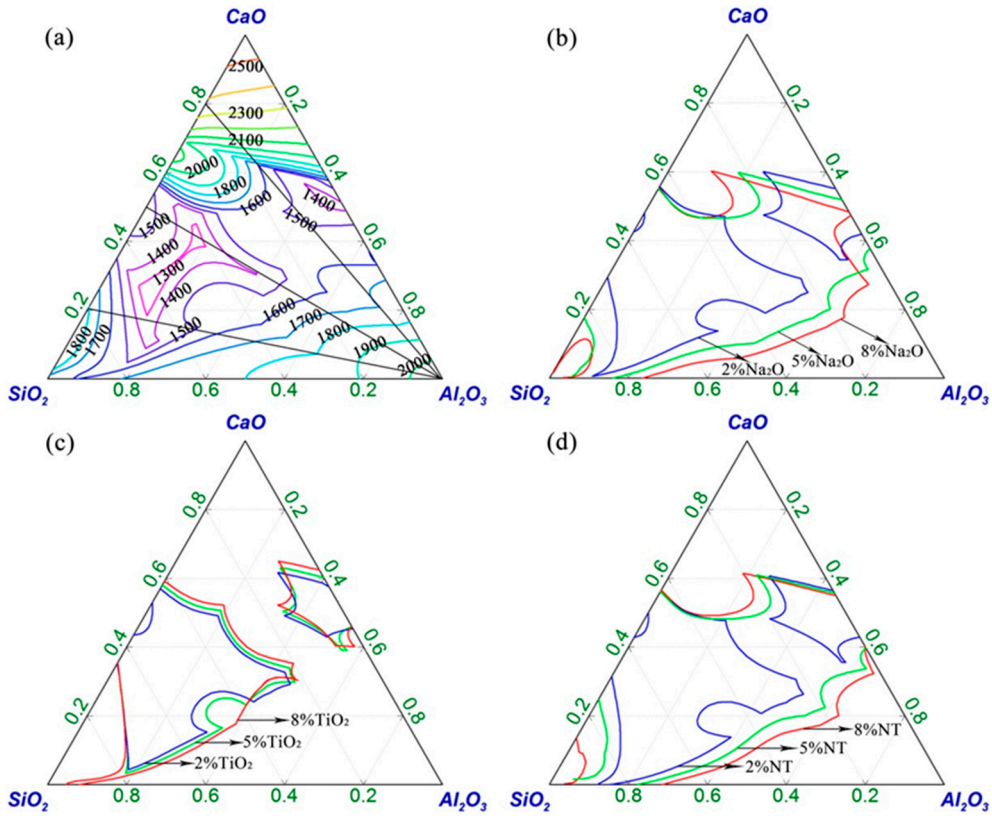

Figure 1. (**a**) Liquid areas of the CaO-SiO_2-Al_2O_3 slag system between 1200 °C and 2600 °C, (**b**) effect of Na_2O on the CaO-SiO_2-Al_2O_3 slag system at 1500 °C, (**c**) effect of TiO_2 on the CaO-SiO_2-Al_2O_3 slag system at 1500 °C, (**d**) effect of NT on the CaO-SiO_2-Al_2O_3 slag system at 1500 °C.

Therefore, when the temperature is relatively low, it is possible to obtain a good melting effect on slag with the addition of Al_2O_3, Na_2O, and TiO_2. For the actual desulfurization capacity of slag systems and the feasibility of hot metal desulfurization using red mud, slag–metal equilibrium experiments were carried out.

3. Experimental

3.1. Experimental Materials

Iron was prepared by melting electrolytic iron (Fe > 99.6%), high-purity FeS, and graphite particles in an induction furnace. The final iron contained 4.0% carbon and 0.3% sulfur. The base slag was obtained by mixing analytical-grade reagents (i.e., CaO, SiO_2, Al_2O_3, Na_2SiO_3, and TiO_2), and its composition varied around the composition of red mud. Na_2SiO_3 was added as a source of Na_2O [6]. With the help of a muffle furnace, CaO, SiO_2, Al_2O_3, and TiO_2 were calcined at 1000 °C for 2 h, and Na_2SiO_3 was roasted at 300 °C for 2 h to remove carbonates and hydroxides prior to use. The base slag was uniformly mixed in an agate mortar and then formed into cylinders with a diameter of 18 mm, at a pressure of 30 MPa for 2 min. The iron samples were shaped into cylinders with a diameter of 18 mm by wire cutting. The weight of the base slag was about 12 g, and that of the iron sample was about 15 g. The mass ratio of slag to metal was 0.8:1. A graphite crucible (OD = 25 mm, ID = 20 mm, H = 30 mm) was employed in the experiment.

3.2. Experimental Scheme

The experiment mainly consisted of two parts. For experiments T1–Ti3, the effect of temperature, basicity (i.e., CaO/SiO_2), and Al_2O_3, Na_2O, and TiO_2 content on the sulfur distribution ratio were measured by changing a single factor. For experiments 1–21, we referred to the method of uniform design [12]. Multiple factors were changed simultaneously, including temperature, basicity, Al_2O_3, Na_2O, and TiO_2 content. The test points were distributed as evenly as possible within the test range, so that each test point could be representative. The slag composition after equilibration is shown in Table 1.

3.3. Experimental Equipment

The experimental equipment included a horizontal resistance furnace, a gas-purification system, and a water-cooling device, whose schematic diagram is shown in Figure 2. A proportional-integral-derivative (PID) controller controlled the furnace with $MoSi_2$ heating elements. After being calibrated, a Pt-30%Rh/Pt-6%Rh thermocouple was used to measure the temperature. The temperature control range of the furnace was 25–1700 °C, and the temperature accuracy of the heating zone was ±2 °C. The water-cooling device was circulated with cooling water to control the temperature at the end of the furnace tube. The gas-purification system consisted of allochroic silica gel, a molecular sieve for dehydration, and copper and magnesium pieces (heated to 500 °C) for deoxidation. Through the gas-purification system, high-purity argon (Ar > 99.99%) was introduced into the horizontal furnace tube to protect the samples and graphite crucibles from being oxidized until the experiment's conclusion.

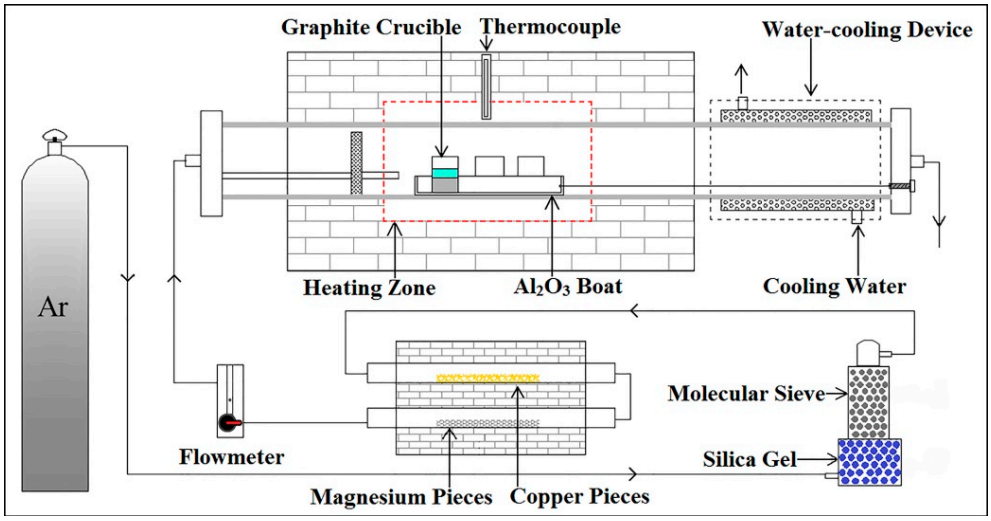

Figure 2. Schematic diagram of the experimental device.

Table 1. Experimental data after equilibration.

No.	Temp./°C	Slag and Metal-Phase Composition (mass%)							Basicity	Λ	L_S	$\log L_S$
		CaO	SiO_2	Al_2O_3	Na_2O	TiO_2	[%S]	(%S)				
T1	1400	48.29	27.87	17.84	1.80	4.20	0.01345	0.3788	1.73	0.7033	28.16	1.4496
T2	1450	48.99	27.99	17.92	0.89	4.21	0.01049	0.3784	1.75	0.7017	36.07	1.5571
T3	1500	49.47	27.70	18.13	0.40	4.30	0.00914	0.3817	1.79	0.7018	41.76	1.6208
R1		39.14	37.17	17.47	2.13	4.09	0.01376	0.3769	1.05	0.6599	27.39	1.4376
R2		48.99	27.99	17.92	0.89	4.21	0.01049	0.3784	1.75	0.7017	36.07	1.5571
R3		54.04	22.29	18.78	0.55	4.34	0.00475	0.3815	2.42	0.7285	80.32	1.9048
A1		51.51	30.22	13.11	0.96	4.20	0.00783	0.3778	1.70	0.7063	48.25	1.6835
A2		48.99	27.99	17.92	0.89	4.21	0.01049	0.3784	1.75	0.7017	36.07	1.5571
A3	1450	46.20	25.97	22.11	1.34	4.38	0.01300	0.3820	1.78	0.6980	29.38	1.4681
N1		49.74	28.38	17.38	0.33	4.17	0.01126	0.3727	1.75	0.7011	33.10	1.5198
N2		48.99	27.99	17.92	0.89	4.21	0.01049	0.3784	1.75	0.7017	36.07	1.5571
N3		48.01	27.44	18.79	1.46	4.30	0.00947	0.3695	1.75	0.7018	39.02	1.5913
Ti1		50.06	28.57	18.11	1.19	2.07	0.00973	0.3718	1.75	0.7049	38.21	1.5822
Ti2		48.99	27.99	17.92	0.89	4.21	0.01049	0.3784	1.75	0.7017	36.07	1.5571
Ti3		48.19	27.39	17.27	0.62	6.53	0.01062	0.3763	1.76	0.6995	35.43	1.5494
1		45.36	27.11	18.66	2.85	6.02	0.01205	0.3762	1.67	0.6997	31.22	1.4946
2		53.86	23.43	13.88	3.41	5.42	0.00671	0.3854	2.30	0.7386	57.44	1.7591
3		42.81	31.01	19.46	2.03	4.69	0.01461	0.3797	1.38	0.6809	25.99	1.4147
4	1400	53.22	26.69	15.78	0.74	3.57	0.01066	0.3733	1.99	0.7177	35.02	1.5444
5		36.00	34.27	22.51	3.50	3.72	0.01864	0.3801	1.05	0.6598	20.39	1.3095
6		47.94	27.35	19.13	2.51	3.07	0.01180	0.3831	1.75	0.7058	32.47	1.5114
7		56.74	24.49	14.77	1.78	2.22	0.00704	0.3778	2.32	0.7388	53.66	1.7294
8		43.07	30.69	19.17	1.14	5.93	0.01328	0.3785	1.40	0.6790	28.50	1.4549
9		50.80	25.66	16.76	0.92	5.86	0.01083	0.3774	1.98	0.7127	34.85	1.5420
10		36.43	33.92	22.06	2.32	5.27	0.02115	0.3793	1.07	0.6576	17.93	1.2536
11	1450	48.99	27.99	17.92	0.89	4.21	0.01049	0.3784	1.75	0.7015	36.07	1.5571
12		58.63	23.87	13.15	0.74	3.61	0.00671	0.3873	2.46	0.7427	57.72	1.7613
13		46.35	31.45	18.91	0.68	2.61	0.01175	0.3827	1.47	0.6856	32.57	1.5128
14		54.27	25.09	15.83	2.29	2.52	0.00746	0.3865	2.16	0.7310	51.81	1.7142
15		39.55	32.00	21.95	0.74	5.76	0.01783	0.3789	1.24	0.6644	21.25	1.3274
16		49.71	27.19	16.98	0.68	5.44	0.00814	0.3731	1.83	0.7050	45.84	1.6611
17		57.58	24.03	13.39	0.26	4.74	0.00672	0.3696	2.40	0.7367	55.00	1.7401
18	1500	44.20	30.36	19.98	0.46	5.00	0.01606	0.3719	1.46	0.6803	23.16	1.3645
19		54.97	25.67	15.06	0.21	4.09	0.00827	0.3744	2.14	0.7237	45.27	1.6560
20		44.44	31.18	21.14	0.39	2.85	0.01289	0.3811	1.43	0.6790	29.57	1.4708
21		54.60	27.13	15.77	0.12	2.38	0.00708	0.3662	2.01	0.7187	51.72	1.7138

3.4. Experimental Procedure

Pre-prepared slag and iron were placed in the graphite crucible. At the same temperature, an Al_2O_3 boat can hold five graphite crucibles simultaneously. They were positioned in the heating zone of the furnace with the help of a molybdenum bar. Ar gas was introduced into the furnace tube at the flow rate of 500 mL/min. The furnace was then switched on. Before this, an experiment had been carried out to determine the equilibrium time. Figure 3 shows the change of sulfur content with time. (i.e., in experiment T1, the mass ratio of slag to metal was 0.3:1.) It was found that the sulfur content was almost unchanged after 4 h. Therefore, an equilibrium time of 4.5 h was chosen to ensure a complete reaction [13,14]. When equilibrium was reached, the Al_2O_3 boat was pulled out of the furnace tube immediately for quenching. After being cooled, the slag and iron were separated. The slag was dried and then crushed into 200 mesh particles. The iron was washed with a steel brush and ultrasonically cleaned to remove surface residues. The sulfur content in slag and iron was detected by a carbon-sulfur analyzer (EMIA-920V2, HORIBA, Kyoto, Japan), and the composition of the slag was determined by an X-Ray fluorescence spectrometer (XRF-1800, Shimadzu, Kyoto, Japan). All experimental results are listed in Table 1.

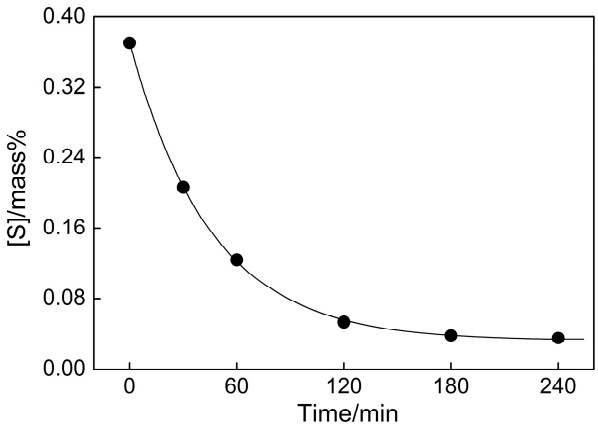

Figure 3. The change of sulfur content in the metal with time.

4. Results and Discussion

4.1. Effect of Temperature

The temperature dependence of $\log L_S$ is shown in Figure 4. The data in Figure 4a are the results of experiments T1–T3, shown in Table 1. For these experiments, the slag compositions were similar. Figure 4b shows the dependence of $\log L_S$ on the temperature for all five components of the slag system (CaO-SiO_2-Al_2O_3-Na_2O-TiO_2), whose compositions varied significantly (i.e., experiments 1–21 in Table 1). As it can be seen from Figure 4a, $\log L_S$ increased from 1.45 to 1.62 when the temperature increased from 1400 °C to 1500 °C, for similar slag compositions. The desulfurization reaction is endothermic. Thus, the high temperature promotes the migration of sulfur from the metal into the slag phase. Simeonov et al. [13] investigated the sulfur distribution ratio between CaO-SiO_2-Al_2O_3-CaF_2 slag and carbon-saturated iron from 1450 °C to 1600 °C and learned that $\log L_S$ increased with the increase in temperature. The value of $\log L_S$ in Simeonov's experiment was much larger than that in this paper, mainly because of the higher basicity in their study. (The basicity in their study was 4.4, whereas, here, it was only about 1.75). Lin et al. [15] measured the sulfur distribution ratio between CaO-SiO_2-Al_2O_3-MgO-TiO_2 slag and carbon-saturated iron from 1450 °C to 1550 °C. The value of $\log L_S$ in Lin's experiment was much larger than that in this paper, because of the low content of weak acid oxides (Al_2O_3 = 10%, TiO_2 = 0–8%).

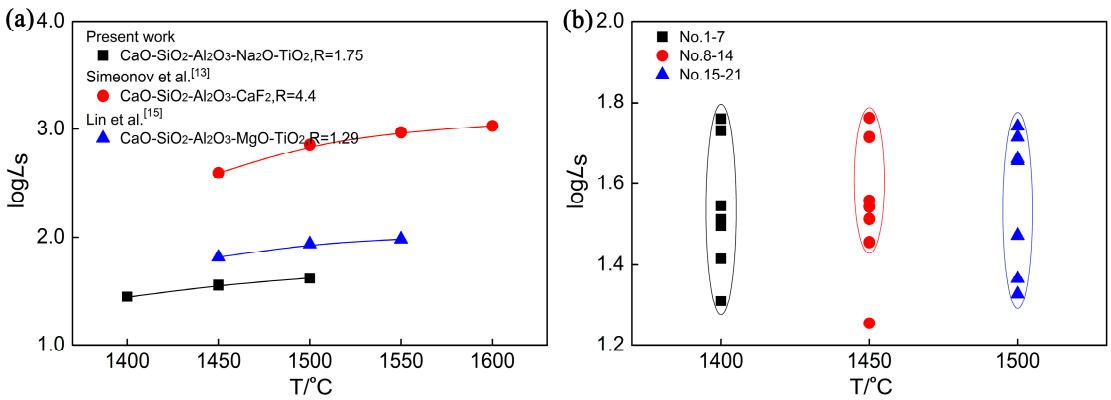

Figure 4. Effect of temperature on logL_S.

However, this trend did not hold for the data shown in Figure 4b, which suggests that the temperature has no significant effect on logL_S when the slag compositions vary significantly. Despite the different requirements of temperature, a similar tendency was observed in the research [16] on the phosphorus distribution ratio between the CaO-FeO-SiO_2-Al_2O_3-Na_2O-TiO_2 slag and the carbon-saturated iron, which suggests that the phosphorus distribution ratio showed much greater dependency on the slag composition, such as on basicity rather than on temperature. Together, these results indicate that, for hot metal pretreatment, slag compositions tend to have significant effects on the desulfurization/dephosphorization efficiency.

4.2. Effect of Basicity

Figure 5a shows the effect of basicity (i.e., CaO/SiO_2) on logL_S. The data are the results of experiments R1–R3, for which the other factors of the slag are similar, but the basicity is different. The value of logL_S increased from 1.44 to 1.90 with an increase in basicity from 1.05 to 2.42. This trend is in accordance with previous research [17–20]. The value of logL_S in Huang's experiments [17] (shown in Figure 5a) was relatively low, mainly because of the high content of weak acid oxides (Al_2O_3 = 15%, TiO_2 = 25%). The increase of basicity implies the disintegration of the silicate network structure [18] and the increase of the free O^{2-} concentration in the slag. A high concentration of free O^{2-} thermodynamically promotes the desulfurization reaction [11].

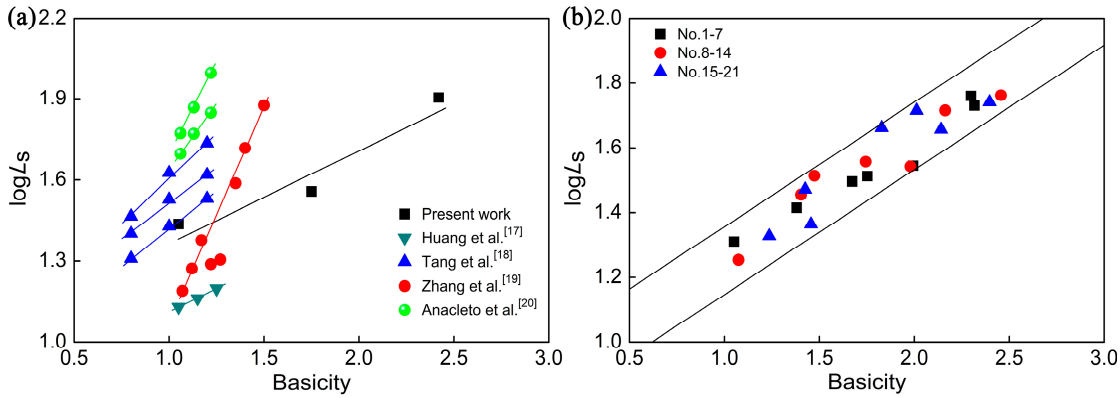

Figure 5. Effect of basicity on logL_S.

The data in Figure 5b are the results of experiments 1–21. The temperature had three gradients, and the composition of slag was changed simultaneously at each temperature. Irrespective of Al_2O_3, Na_2O, and TiO_2 content and temperature, logL_S showed a strong dependence on the basicity of the slag, which linearly increased with the increase in basicity. This suggests that basicity has a much stronger effect on logL_S than other influencing factors, such as temperature, under this experimental condition.

4.3. Effect of Al_2O_3

Figure 6a shows the effect of Al_2O_3 content on $\log L_S$. The data are the results of experiments A1–A3, for which all slag factors were similar, with the exception of Al_2O_3 content. As can be seen, the value of $\log L_S$ decreased from 1.68 to 1.47 with an increase in Al_2O_3 content from 13.11% to 22.11%. This was due to the fact that Al_2O_3 acted as an acidic oxide in the basic slag. Al_2O_3 consumed the free O^{2-} to form $[AlO]_4^{5-}$-tetrahedron, which decreased free O^{2-} concentration and weakened the desulfurization capacity of the slag [21]. The same experimental trend was observed by Zhang et al. [19]. They obtained a much lower sulfur distribution ratio, even at a higher temperature (1500 °C), than the present work (1450 °C), mainly because of the lower basicity (1.17) of the slag in their study.

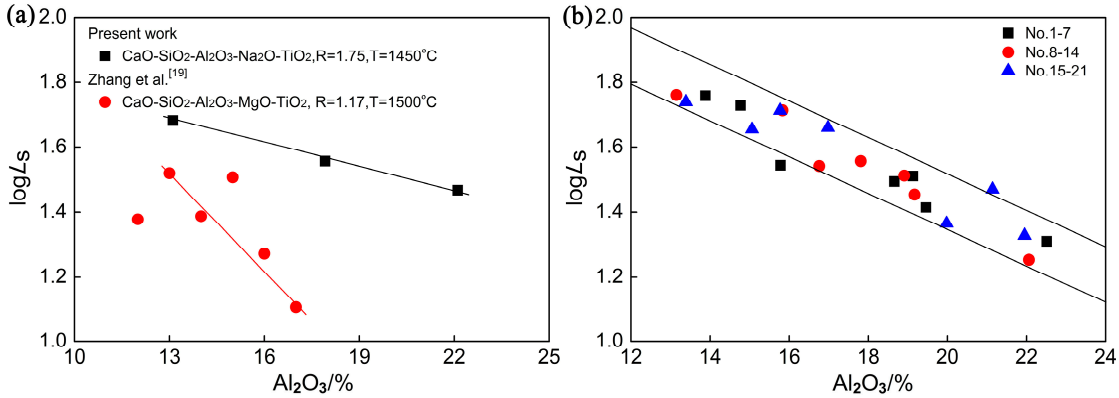

Figure 6. Effect of Al_2O_3 on $\log L_S$.

The data in Figure 6b are the results of experiments 1–21. The temperature had three gradients, and the composition of slag was changed simultaneously at each temperature. Irrespective of basicity, Na_2O and TiO_2 content, and temperature, $\log L_S$ also showed a strong dependence on Al_2O_3 content. This suggests that Al_2O_3 is also an important factor affecting the sulfur distribution ratio under this experimental condition.

4.4. Effect of Na_2O

Figure 7a shows the effect of Na_2O content on $\log L_S$. The data are the results of experiments N1–N3, for which the other factors of the slag are similar. As can be seen, $\log L_S$ linearly increased from 1.52 to 1.59, with an increase in Na_2O content from 0.33% to 1.46%. This was because Na_2O is a strong basic oxide, and Na^+ tends to have a strong affinity for S^{2-}. Niekerk et al. [5] pointed out that the addition of Na_2O significantly increased the sulfide capacity of silicate and lime-based slag. Additionally, the Na_2O equivalent of CaO was determined to be 0.30. Pak and Fruehan [6,22] suggested that Na_2O could lower the melting point of a lime-based slag, reduce the consumption of acid oxides to CaO, and significantly increase the activity of CaO. Subsequently, the desulfurization capacity of the slag was enhanced.

The data in Figure 7b are the results of experiments 1–21. The temperature had three gradients, and the composition of the slag was changed simultaneously at each temperature. When other factors (e.g., temperature) changed, Na_2O content in the slag had no significant effect on $\log L_S$. This could be due to the experimental conditions. Because of the strong reduction potential of hot metal, Na_2O can be reduced to metal Na, which can easily evaporate into the gas phase, especially at a high temperature. Therefore, the higher the temperature, the more Na vaporizes into the gas phase, and less residual Na_2O content remains in the slag. As shown in Figure 7b, the Na_2O content was 0.74–3.50% (square symbols in Figure 7b) at the lower temperature (1400 °C), while at a high temperature (1500 °C), the Na_2O content was only 0.12–0.74% (triangular symbols in Figure 7b). The promoting effect on desulfurization of higher Na_2O content was eventually counteracted by lower temperatures, as in

the case where the negative influence of lower Na_2O content tended to be neutralized by higher temperatures. Comprehensively, Na_2O content showed no significant effect on $\log L_S$ under this experimental condition.

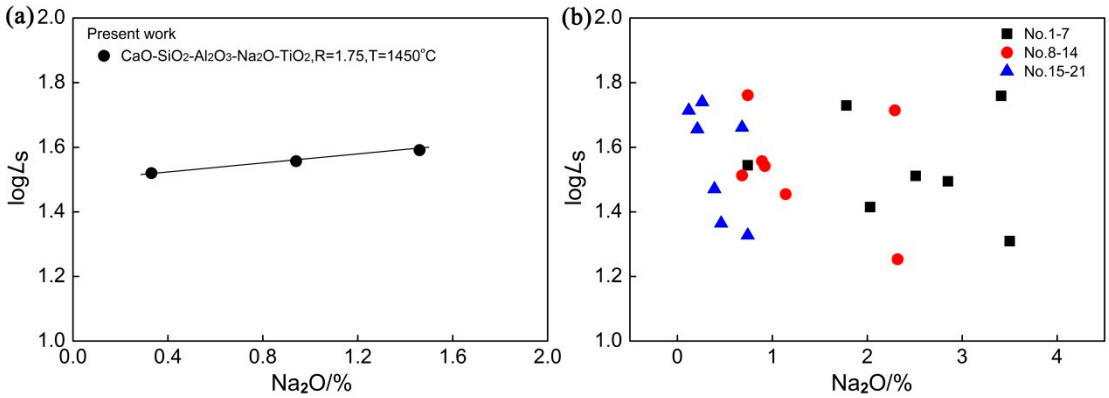

Figure 7. Effect of Na_2O on $\log L_S$.

However, a different tendency was observed in the case of hot metal dephosphorization. The results of hot metal dephosphorization by Li [16] showed that, when changing various factors, such as temperature and slag compositions, the distribution ratio of phosphorus between the slag and iron-saturated iron (L_P) increased significantly with the increase of Na_2O content. This was mainly because hot metal dephosphorization was carried out in an oxidizing atmosphere, and Na_2O in the slag was hard to be reduced to metal Na. The volatilization of Na_2O is much weaker than that of metal Na. Finally, more Na_2O is maintained, and it plays the role of a strong basic oxide in the slag phase. Consequently, hot metal dephosphorization is promoted by high Na_2O content.

4.5. Effect of TiO_2

Figure 8a shows the effect of TiO_2 content on $\log L_S$. The data are the results of experiments Ti1–Ti3, for which all factors of the slag were similar except for TiO_2 content. As can be seen, the value of $\log L_S$ decreased slightly from 1.58 to 1.55 with an increase in TiO_2 content from 2.07% to 6.53%. This is in accord with the results of Lin et al. and Tang et al. [15,18], who investigated the sulfur distribution ratio between $CaO\text{-}SiO_2\text{-}Al_2O_3\text{-}MgO\text{-}TiO_2$ slag and carbon-saturated iron at 1500 °C. The electrostatic potential of Ti^{4+} (5.88) is lower than that of Si^{4+} (9.76). Therefore, the Ti-O bond is weaker than the Si-O bond, which causes TiO_2 to exist as $[TiO]_6^{8-}$-octahedron in a basic slag. Sommerville et al. [23] also suggested that TiO_2 acted as an acidic oxide in a basic slag and existed in the form of $[TiO]_6^{8-}$-octahedron, which decreased the amount of free O^{2-} and weakened the desulfurization capacity of the slag.

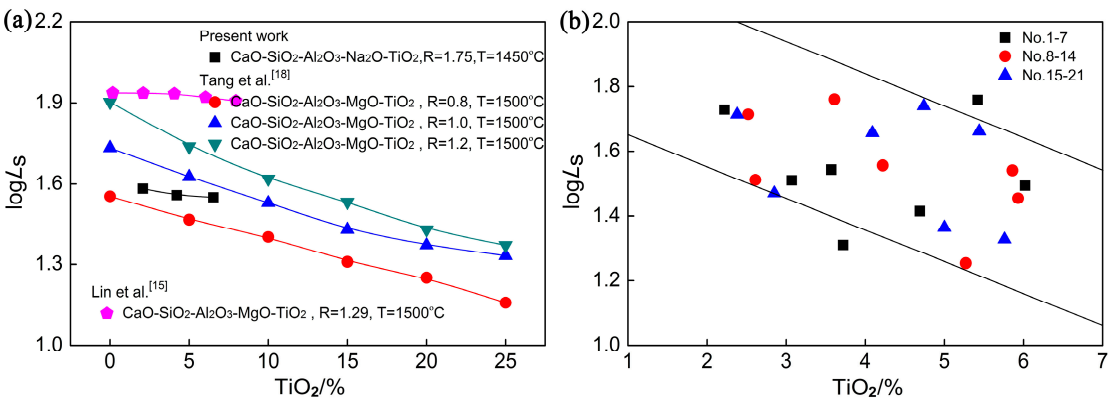

Figure 8. Effect of TiO_2 on $\log L_S$.

The data in Figure 8b are the results of experiments 1–21. The temperature had three gradients, and the composition of the slag was changed simultaneously at each temperature. Although a relatively large fluctuation was observed, the total logL_S decreased with an increase in the TiO_2 content. This indicates that TiO_2 in the slag has also a thermodynamically negative effect on the desulfurization capacity of the slag.

4.6. Regression Analysis of logL_S

To further study the relationship between logL_S, Λ, and T, based on the data of experiments 1–21 in Table 1, the following regression equation was obtained by using the SPSS (Statistical Product and Service Solutions) software (SPSS10.91, SPSS Inc., Chicago, IL, USA) [24]. A comparison between the experimental values and the calculated values of logL_S is shown in Figure 9, which shows good agreement.

$$\log L_S = 15.584\Lambda + \frac{10568.406 - 17184.041\Lambda}{T} - 8.529, \ (\mathrm{r} = 0.963) \quad (1)$$

where L_S is the sulfur distribution ratio; T is the temperature, °C; Λ is the optical basicity of the slag [25]; r denotes the correlation coefficient.

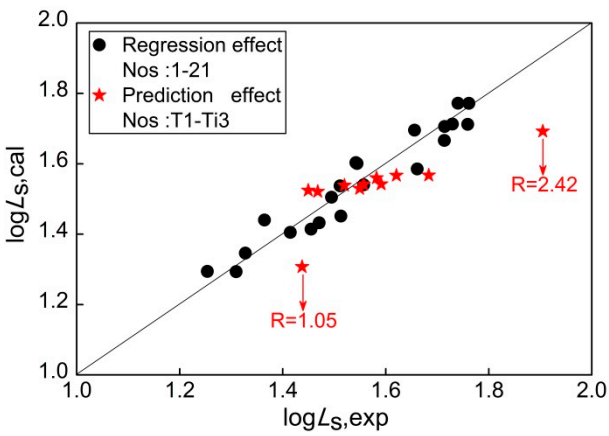

Figure 9. Comparison of experimental values and calculated values.

When the temperature was 1400–1500 °C, basicity was 1.0–2.5, Al_2O_3 content was 12–22%, Na_2O content was 0–3%, and TiO_2 content was 2–6%. The equation could be helpful in predicting the sulfur distribution ratio between CaO-SiO_2-Al_2O_3-Na_2O-TiO_2 slag and carbon-saturated iron.

5. Conclusion

The sulfur distribution ratio between CaO-SiO_2-Al_2O_3-Na_2O-TiO_2 slag and carbon-saturated iron was re-evaluated in this study. Based on the theoretical calculation and equilibrium experiments, the conclusions are summarized as follows.

(1) The thermodynamic calculation shows that high temperature helps the melting of the slag. Al_2O_3 is beneficial as a flux. However, the content should be controlled. Na_2O can promote the melting effect on the slag more effectively than TiO_2.

(2) The experimental data suggest that the distribution ratio of sulfur between the slag and the carbon-saturated iron strongly increases with the increase of temperature, basicity, and Na_2O content, whereas it decreases with the increase of Al_2O_3 and TiO_2 content. Na_2O in the slag will volatilize because of the high temperature and the reducing conditions.

(3) Based on the experimental data, for the distribution ratio of sulfur between CaO-SiO_2-Al_2O_3-Na_2O-TiO_2 slag and carbon-saturated iron, the following fitting formula is obtained:

$$\log L_S = 15.584\Lambda + \frac{10568.406 - 17184.041\Lambda}{T} - 8.529$$

Author Contributions: K.Z. and Y.Z. designed the experiments; K.Z. performed the experiments, analyzed the data, and compiled the text; T.W. reviewed the manuscript.

Funding: The authors would like to acknowledge the financial support of National Key R&D Program of China (No. 2017YFC0210301) and the National Natural Science Foundation of China (No. 51474021) for this work.

Conflicts of Interest: The authors declare no conflict of interest.

References

1. Mohassab-Ahmed, M.Y.; Sohn, H.Y.; Kim, H.G. Sulfur distribution between liquid iron and magnesia-saturated slag in H_2/H_2O atmosphere relevant to a novel green ironmaking technology. *Ind. Eng. Chem. Res.* **2012**, *51*, 3639–3645. [CrossRef]
2. Iwamasa, P.K.; Fruehan, R.J. Effect of FeO in the slag and silicon in the metal on the desulfurization of hot Metal. *Metall. Mater. Trans. B* **1997**, *28*, 47–57. [CrossRef]
3. Gandarias, A.; Lopez de Lacalle, L.N.; Aizpitarte, X.; Lamikiz, A. Study of the performance of the turning and drilling of austenitic stainless steels using two coolant techniques. *Int. J. Mach. Mach. Mater.* **2008**, *3*, 1–17. [CrossRef]
4. Rodríguez, A.; Lopez de Lacalle, L.N.; Calleja, A.; Fernández, A.; Lamikiz, A. Maximal reduction of steps for iron casting one-of-a-kind parts. *J. Clean. Prod.* **2012**, *24*, 48–55. [CrossRef]
5. Van Niekerk, W.H.; Dippenaar, R.J. Thermodynamic aspects of Na_2O and CaF_2 containing lime-based slags used for the desulphurization of hot-metal. *ISIJ Int.* **1993**, *33*, 59–65. [CrossRef]
6. Pak, J.J.; Fruehan, R.J. The effect of Na_2O on dephosphorization by CaO-based steelmaking slags. *Metall. Mater. Trans. B* **1991**, *22*, 39–46. [CrossRef]
7. Zhang, Y.; Li, F.; Wang, R.; Tian, D. Application of bayer red mud-based flux in the steelmaking process. *Steel Res. Int.* **2017**, *88*, 304–313. [CrossRef]
8. Yajima, K.; Matsuura, H.; Tsukihashi, F. Effect of simultaneous addition of Al_2O_3 and MgO on the liquidus of the CaO-SiO_2-FeO_x system with various oxygen partial pressures at 1573 K. *ISIJ Int.* **2010**, *50*, 191–194. [CrossRef]
9. Chan, A.H.; Fruehan, R.J. The sulfur partition ratio with Fe-C_{SAT} melts and the sulfide capacity of CaO-SiO_2-Na_2O-(Al_2O_3) slags. *Metall. Mater. Trans. B* **1989**, *20*, 71–76. [CrossRef]
10. Park, H.; Park, J.Y.; Kim, G.H.; Sohn, I. Effect of TiO_2 on the viscosity and slag structure in blast furnace type slags. *Steel Res. Int.* **2012**, *83*, 150–156. [CrossRef]
11. Sohn, I.; Wang, W.; Matsuura, H.; Tsukihashi, F.; Min, D.J. Influence of TiO_2 on the viscous behavior of calcium silicate melts containing 17 mass% Al_2O_3 and 10 mass% MgO. *ISIJ Int.* **2012**, *52*, 158–160. [CrossRef]
12. Fang, K.T.; Wang, Y. *Number-Theoretic Methods in Statistics*; CRC Press: Boca Raton, FL, USA, 1993.
13. Simeonov, S.R.; Ivanchev, I.N.; Hainadjiev, A.V. Sulphur equilibrium distribution between CaO-CaF_2-SiO_2-Al_2O_3 slags and carbon-saturated Iron. *ISIJ Int.* **1991**, *31*, 1396–1399. [CrossRef]
14. Tsao, T.; Katayama, H.G. Sulphur distribution between liquid iron and CaO-MgO-Al_2O_3-SiO_2 slags used for ladle refining. *ISIJ Int.* **1986**, *26*, 717–723. [CrossRef]
15. Lin, Y.; Yin, W. Desulfurization ability of the blast furnace slag with low titanium oxide content. *Iron Steel.* **1987**, *22*, 4–9. [CrossRef]
16. Li, F.; Li, X.; Yang, S.; Zhang, Y. Distribution ratios of phosphorus between CaO-FeO-SiO_2-$Al_2O_3/Na_2O/TiO_2$ slags and carbon-saturated iron. *Metall. Mater. Trans. B* **2017**, *48*, 2367–2378. [CrossRef]
17. Huang, Z.; Yang, Z.; Guo, T. Effect of MgO in blast furnance type slags containing TiO_2 on slag desulpurization. *J. Northeast Univ. Nat. Sci.* **1987**, *3*, 335–339.
18. Tang, X.; Xu, C. Sulphur distribution between CaO-SiO_2-TiO_2-Al_2O_3-MgO slag and carbon-saturated iron at 1773 K. *ISIJ Int.* **1995**, *35*, 367–371. [CrossRef]

19. Zhang, J.; Lv, X.; Yan, Z.; Oin, Y.; Bai, C. Desulphurisation ability of blast furnace slag containing high Al_2O_3 and 5 mass% TiO_2 at 1773 K. *Ironmak. Steelmak.* **2016**, *43*, 378–384. [CrossRef]
20. Anacleto, N.M.; Lee, H.-G.; Hayes, P.C. Sulphur partition between CaO-SiO_2-Ce_2O_3 slags and carbon-saturated iron. *ISIJ Int.* **1993**, *33*, 549–555. [CrossRef]
21. Park, J.H.; Min, D.J.; Song, H.S. Amphoteric behavior of alumina in viscous flow and structure of CaO-SiO_2(-MgO)-Al_2O_3 slags. *Metall. Mater. Trans. B* **2004**, *35*, 269–275. [CrossRef]
22. Pak, J.J.; Ito, K.; Fruehan, F.J. Activities of Na_2O in CaO-based slags used for dephosphorization of steel. *ISIJ Int.* **1989**, *29*, 318–323. [CrossRef]
23. Sommerville, I.D.; Bell, H.B. The behaviour of titania in metallurgical slags. *Can. Metall. Q.* **1982**, *21*, 145–155. [CrossRef]
24. Yockey, R.D. *SPSS Demystified: A Step by Step Approach*; Prentice Hall: Upper Saddle River, NJ, USA, 2010.
25. Yang, Y.D.; Sommerville, I.D.; McLean, A. Some fundamental considerations pertaining to oxide melt interactions and their influence on steel quality. *Trans. Indian Inst. Met.* **2006**, *59*, 655–669.